

Review

Towards 30% Efficiency by 2030 of Eco-Designed Building Integrated Photovoltaics

Nikolaos Skandalos ^{1,*}, Vasileios Kapsalis ², Tao Ma ³ and Dimitris Karamanis ^{4,*}

¹ University Centre for Energy Efficient Buildings, Czech Technical University in Prague, 1024 Třinecká St., 27343 Buštěhrad, Czech Republic

² Sector of Industrial Management and Operational Research, School of Mechanical Engineering, National Technical University of Athens, 9 Heroon Polytechniou Str., Zografou Campus, 15780 Athens, Greece; bkapsal@mail.ntua.gr

³ School of Mechanical Engineering, Shanghai Jiao Tong University, Shanghai 200240, China; tao.ma@sjtu.edu.cn

⁴ Department of Environmental Engineering, University of Patras, 2 Georgiou Seferi St., 30100 Agrinio, Greece

* Correspondence: nikolaos.skandalos@cvut.cz (N.S.); dkaraman@upatras.gr (D.K.)

Abstract: The necessity of affordable and durable building-integrated photovoltaics has gained widespread importance for the renewable energy transition involving electrification and decarbonization in climate-neutral cities that possess many public health co-benefits. Although the PV market is dominated by polycrystalline and monocrystalline silicon solar cells of the first generation, there is an impetus in the research lately for more sophisticated solar cell architectures with higher efficiency, longer lifetime, and less use of raw materials in an eco-design approach. To accelerate building integration of the next generation of photovoltaics and the associated climate change mitigation benefits, we propose in this work a holistic novel approach to the requirements and associated parameters for the emerging and innovative PV structures, spanning from intrinsic cell properties to panels effect in the urban environment. Within this framework, and supported by building simulation, the improvement of cells' efficiency is revealed as an important parameter for their wider PV building and urban deployment as well as a major improvement in covering the building energy needs with minimized thermal impact in the urban environment. By analyzing the lab-reported values and the timeline of emerging and novel tandem solar cells, we propose the 30% BIPV efficiency of the eco-designed BIPV products as a central milestone to be attained before 2030 for a sustainable urban transformation.

Keywords: solar cells; power conversion efficiency; eco-design; building integrated photovoltaic; BIPV; sustainable urban transformation



Citation: Skandalos, N.; Kapsalis, V.; Ma, T.; Karamanis, D. Towards 30% Efficiency by 2030 of Eco-Designed Building Integrated Photovoltaics. *Solar* **2023**, *3*, 434–457. <https://doi.org/10.3390/solar3030024>

Academic Editor: Javier Muñoz Antón

Received: 29 June 2023

Revised: 17 July 2023

Accepted: 4 August 2023

Published: 7 August 2023



Copyright: © 2023 by the authors. Licensee MDPI, Basel, Switzerland. This article is an open access article distributed under the terms and conditions of the Creative Commons Attribution (CC BY) license (<https://creativecommons.org/licenses/by/4.0/>).

1. Introduction

Although there have been considerable research efforts in recent years toward the clean energy transition, there are still barriers to overcome for a 100% adaptation to renewable energy. Cities are responsible for more than 70% of the total CO₂ emission, and deep decarbonization is required due to local heat islands [1] which are enhanced by regional and global climate change effects. Several recent studies [2,3] report that the temperature increase in the cities has been raised dangerously over the last decade, with more heatwaves expected to appear in coming years. The number of premature deaths is estimated to be more than six thousand in major European cities due to the effects of Urban Heat Islands (UHIs) during summer [4]. Moreover, two more solutions are being investigated to mitigate the impact, increase the greenery (e.g., 30% trees would decrease the mortality), and reduce the time spent indoors (e.g., by working four days). However, technology is responsible for the situation and should, in principle, be able to provide a solution to the problem created, in addition to nature-based solutions and energy needs reduction.

Among the different technological solutions proposed to mitigate the phenomenon, we have recently shown that building integrated photovoltaics (BIPVs) can generate enough electricity to cover all the building energy needs towards net zero energy buildings in global climate conditions [5]. In this context, buildings' residents and cities can be transformed into prosumers and citizens of solar cities, respectively. Although the BIPV market is expanding, an annual growth rate of 25% is required from 2022 to 2030 to increase the current 1000 TWh electricity generation to 7400 TWh in 2030 and be on track for climate change mitigation [6]. This vast increase will require an investment of more than \$320B within the next seven years in PV costing 0.01 \$/kWh, and necessitate reaching a capacity of more than 5 TW globally. With the new installations, the share of residential PV is expected to be higher than in 2021 at 28%, corresponding to 1.4 TW of installed photovoltaics. In EU-27, 41.4 GW of new grid-connected photovoltaics was installed in 2022, representing a 47% increase from 2021.

PV cumulative installation has been astonishing in the last few years, and their deployment is at the center of the energy transition. With the cost of the PV module decreasing considerably, the largest amount of PV cost deployment is related to the soft cost attributed to land acquisition use, developer overheads, governmental taxes, and installation work [7]. As a result of landscape sharing and biodiversity loss, the challenge is to accelerate innovation and city PV deployment so that cities can substantially reduce greenhouse gas emissions and be more sustainable and equitable [8].

Building integration of photovoltaics appeared in the 1970s and can be considered as PV installations over the existing building exterior or as essential building components, regularly serving as the skin interface with the external building environment [5]. The majority of the BIPV applications were based on the use of the technology of the first generation of crystalline silicon cells (Figure 1) and the second generation of thin films as amorphous silicon (a-Si) semi-transparent glazings. The latter are more expensive to produce and operate at lower efficiencies. With the advent of the third generation of photovoltaics, more solar cell architectures have been successfully integrated in the building environment, such as organic transparent photovoltaic windows [9], CIGS [10], halide perovskites [11], 2T perovskite/silicon tandem BIPV [12].

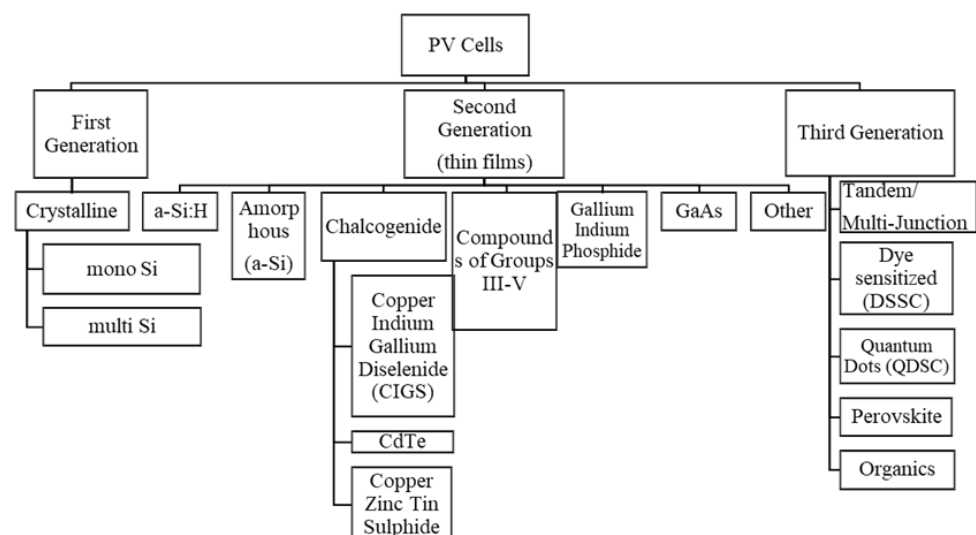


Figure 1. Generations of solar cells for building integrated photovoltaics.

However, the PV building integration is being delayed globally As a result of architectural adaptation and difficulties in stakeholders' and end-users' engagement with its subsequent adoption. Moreover, BIPV deployment is hindered As a result of important additional barriers, which are climate and space dependent and difficult to resolve.

Furthermore, rooftop photovoltaics (RTPVs) have effectively covered the electricity needs of well-insulated and low-rising buildings in net zero energy buildings [13]. With

the energy needs of passive houses at around 50 kWh/m²/Y (year), half coverage of a typical 140 m² roof can electrify (including heating) a 4-floor building in a moderate climate. However, there are four limitations to this condition: (a) the increase in RTPV deployment in the built environment has raised considerable concerns on a feedback loop mechanism for urban heat rejection either outdoors through PV surface cooling by convection or from indoors by heat pumping with electrified HVAC systems [14], (b) the lack of economic support on RTPV deployment and availability of local grids to handle the intermittent nature of solar energy, (c) the need to cover an even higher percentage of energy needs for RTPV deployment due to the use of electric vehicles and the increased costs of complementary building integrated photovoltaic (BIPV) solutions, (d) the need that will arise at the end of the decade to replace the RTPV already installed due to its lower efficiency and higher degradation rates. The influence of these limitations could be significantly reduced with the increase in RTPV efficiency in the next generation of photovoltaics for the building environment.

Moreover, there have been review studies with the most comprehensive overview of the different BIPV producers and products reported by Jelle et al., 2012 [15]. However, the evaluation was mainly focused on the most suitable BIPVs for various purposes, while the review of the technological PV developments for BIPVs purposed the last decade is limited. In this context, the present study aims to update the BIPV potential solutions of higher efficiency, focusing on the feasibility of reaching the milestone of 30% efficiency of BIPV products by 2030.

2. Methods

This work delves into the exciting realm of photovoltaics and explores the possibilities for enhancing solar energy conversion through higher efficiencies. As the demand for clean and sustainable energy continues to grow, the frequency of BIPV in the global scientific research literature indicates the relative importance of technology in the research community. Thus, developing eco-designed BIPVs and enhancing their conversion efficiency becomes increasingly crucial. The articles were initially screened to select both experimental and simulation studies focusing on material development and fundamental physical properties science. A range of potential solutions that hold promise in advancing the field of PV technology were examined. From novel materials and advanced cell architectures, our primary aim is to shed light on the path toward achieving 30% efficiency and contribute to the wider adoption of solar energy in the building sector.

Subsequently, to show the necessity of higher efficiencies, a typical 3-floor building in climate conditions resembling central Europe was used to simulate energy needs and compare it with the energy generated by the rooftop PV system. A building model with a core and four perimeter zones, as described by the US Department of Energy for medium-size office buildings (Figure 2), was modeled and simulated in EnergyPlus, while taking into account the shading effect from PV arrays [13]. Then, some local adjustments were made to fit the existing building codes (Table 1). The simulation was performed for a semi-continental climate (Prague) of moderate Global Horizontal Irradiance (GHI) according to our previous study [5].

The simulation of the rooftop PV system was done in PV*SOL, a leading software used by planners, architects, and installers for the design and simulation of PV systems in buildings. In this case, high-performance PV modules were used, the characteristics of which are presented in Table 2. The shading of arrays can significantly impact PV performance, and thus careful selection of the PV tilt angle and spacing is needed to prevent self-shading and maximize the utilization of the available roof area. In this study, a conservative value of 0.65 roof cover ratio was used. Finally, hourly profiles and other metrics related to PV performance were simulated and used for the assessment of the net energy performance of the building.

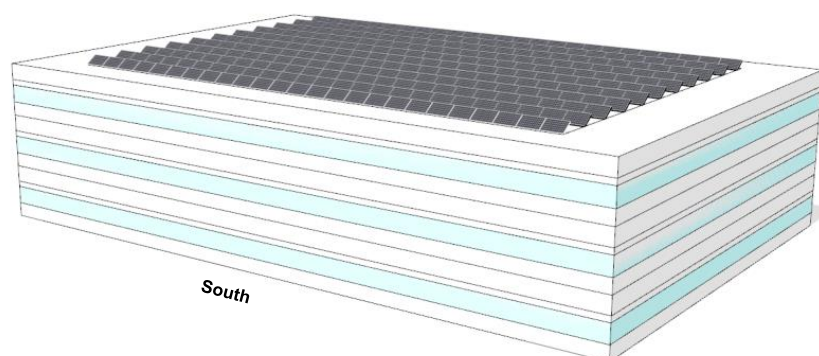


Figure 2. 3D model of the medium-sized office building obtained from DOE and the rooftop PV system.

Table 1. The case study building envelope and simulation parameters.

Parameter	Value
Floor U-value	0.45 W/m ² K
External wall U-value	0.3 W/m ² K
Roof U-value	0.24 W/m ² K
Roof albedo	0.25
Double glazing unit	U-value [W/m ² K] = 1.493, SHGC = 0.373, T _{vis} = 0.444
Airtightness	0.35 ACH
Operation	8 AM–6 PM (weekdays)
Heating occupied set-point	21 °C (15.6 °C unoccupied)
COP heating system	3 (heat pump)
Cooling occupied set-point	24 °C (26.7 °C unoccupied)
COP cooling system	3 (heat pump)
Mechanical ventilation	8 L/s/prs
People density	18.5 m ² /prs
Max equipment gains	8.07 W/m ² (variable)
Lighting	10.7 W/m ² (with 500 lx target illuminance)

Table 2. The PV characteristics of the selected commercial module in PVSOL.

Parameter	Value
PV module dimensions	1134 mm × 1762 mm
PMPP	440 W
VMPP	44 V
IMPP	10 A
Module efficiency	22%
Temperature coefficient of P _{MAX}	−0.30%/°C
Total installed capacity	146 kWp
PV tilt angle	15°
Specific annual yield	1042 kWh/kWp
Performance ratio	91.5%

3. Building Integrated PV

3.1. Requirements and Characteristics of BIPV and Built Environment Integrated PV

The physical integration of photovoltaics into the building and infrastructure environment includes building integration (BIPV), agrivoltaics and landscape integration (ALIPV), and floating PV integrated into the urban water bodies (FWBPV). The module patterning PV permits their city integration in a variety of different building surfaces and urban spaces from the building rooftop, facade, walls, windows, and inclined surfaces of architectural additions as shadings to urban photovoltaics as parking lots, advertising boards, and artificial street and public square PV trees. Due to the drastic reduction in module cost and

solar policy incentives, photovoltaics have shown tremendous growth during past decades with the fastest learning rate among other forms of energy generation, and their integration in the urban environment is mandatory for a successful and sustainable energy transition in cities worldwide. Concepts such as zero-energy buildings, positive energy districts, and carbon-neutral cities have gained public acceptability and are being implemented in several demonstration projects worldwide.

Successful use and visualization of BIPV projects globally are shown in Figure 3, while recent reviews have comprehensively analyzed the barriers and challenges in their wider deployment [5,16] (Table 3). Since the decarbonization process will be based on photovoltaics, their environmental impact, in addition to that of the associated electronics, should be minimized throughout their life cycle. Eco-design practices in BIPV systems are essential for maximizing sustainability, minimizing environmental impact, and advancing the transition toward a circular and sustainable energy future. Eco-design involves considering environmental factors during the design phase of BIPV systems, such as using sustainable and environmentally friendly materials with durability and resistance to degradation. By integrating these principles throughout the life cycle of BIPV systems, from manufacturing to end-of-life management, eco-design can significantly reduce their environmental footprint. This is the main scope of the eco-design labeling of a product, with an energy-labeling scheme proposed recently by [17]. European PV manufacturing companies pay particular attention to PV eco-labeling by introducing an Environmental Impact Index especially for residential systems [18]. New regulation by the European Commission, in PV eco-design and energy labeling measures within the management of the environmental impacts of photovoltaic products, is planned for the fourth quarter of 2023 [19].



Figure 3. Successful use and visualization of BIPV projects globally. From top and left to right, CIS tower in Manchester by Pit-yacker, Photovoltaic Facade in Barcelona, public domain. From bottom and left to right: Solar facade in Madrid by Hanjin, Apple RTPV Park by Daniel L. Lu (all photos under open-access license).

Table 3. Barriers and challenges in BIPV deployment [5,16].

Challenges	Overcome Barriers
Dual Use Issues, energy generator, and building component	BIPV integration in the building management tools
Operating conditions and high cell temperature	The development of safety within certification practices
Refurbishment but versatility in colors, transparency, and design	Development of novel BIPV technologies such as perovskite and third-generation solar cells
Fire safety	BIPV certification, eco, and energy labeling
Reliability and quality of architectural integration	Adaptation to market requirements through customization, energy performance, and economic aspects
Outdoor performance	Improving the maintenance and operation procedures
Issues with technology development	Dissemination of best practices
Ability to replace BIPV components	Reducing public doubt of the technology with neighborhood installation
Standardization of BIPV components	Common utility resource and not a product
Training by trades	Synergistic positive effect with nature-based solutions such as greenery

In their large-scale adoption, PV modules for building integration should satisfy the building construction products as have been in the European Construction Product Regulation CPR 305/2011 based on technical, mechanical, and weathering properties; total protection from natural and accidental risks as fire, health, safety and security; accessibility in use; environmental rating; protection against noise; energy economy and heat retention; and sustainable use of natural resources [20]. These are basic requirements for BIPVs as construction products and integration works, while IEC requirements are also mandatory as active components for electricity generation. Regarding their function, the surface of the deployment area, the orientation, the design, and the technical characteristics of the BIPV components, more regulations and required standards are imposed [21]. Additionally, BIPV bioclimatic design with the sequence of PV integration can be characterized by wider performance criteria [5]. A set of indicative BIPV requirements at different scales and associated parameters are shown in Table 4. Among the most critical parameters of this table is the efficiency of the solar cell technology, since its value can influence many interdependent parameters, such as the cost of BIPV integration and the urban effects of the BIPV surroundings.

With the current PV technology in urban applications, a maximum of around 20% of solar irradiation is converted to useful electricity, while the rest is mainly transferred into the environment as radiation and sensible heat. Despite generating electricity, the waste energy of integrated photovoltaics in the surrounding built and urban environment is higher than other urban overheating mitigation methods, such as green roofs (heat transferred in the environment is less than 60% with indirect benefits but without electricity production) or cool roofs (with almost 90% reflected back to the atmosphere but with penalties in the winter).

In this context, progressing the commercial BIPV efficiency to 30% is a major improvement in addition to extending their lifetime for advancing both the building energy sufficiency requirements and highly reducing the potential overheating issues with large-scale BIPV deployment, especially in hot climates. The importance of the BIPV efficiency increase to 30% by 2030 as a milestone can also be understood by the corresponding per capita installation needs which will be reduced by more than 20%, compared to that projected until 2050 (1.4 to 8 kW per capita [22]). This reduction is significant for low-income or vulnerable residents and developing countries that are incapable of fastening PV building uptake due to the lack of covering basic and priority needs.

Table 4. A holistic approach to the requirements and associated parameters for building integrated photovoltaics.

BIPV Requirements	Category	Characteristics-Parameters
Intrinsic scientific and technological	Solar cell architecture	Generation
		Number of p-n junctions
	Performance	Power conversion efficiency
		Power output
		Temperature coefficient
		Transparency
		Degradation rate
		Lifetime
	Sustainability	Resources abundance
		Embodied energy
		Recycling
		Non-Toxicity (human/ecosystems)
		Climate Impact as g CO ₂ /kW
	Manufacturing materials and complexity	Technology Readiness Level
Raw and critical materials		
Basic as construction product and work	Mechanical	Cost
		Dimensions and Weight
		Flexibility
	Safety	Strength
		Health
		Fire
		Risk
		Security
	Weathering	Accessibility in use
		Maintenance (management, monitoring, cleaning)
		Resistance and Replacement
	Product	Cost
		Eco-designed and Recycling
	Place	Global Horizontal Irradiation
Sunshine duration		
Building	Use-Typology	
	Plan shape-Orientation	
Spatial and energy performance	Integration	Roof
		Facade
		Shading
	Energy performance	Window
		Component
Energy performance	Electricity generation	
	Reduction in H and C energy needs	
	Ventilation	
	Flexibility-Sufficiency-NZEB	
		LCOE

Table 4. *Cont.*

BIPV Requirements	Category	Characteristics-Parameters
Architectural and aesthetical	Aesthetics aspects	LESO-QSV
	Bioclimatic design	BIPV climatic design according to the Koppen-Geiger-GHI classification
	Comfort	Acoustic
		Thermal
	Practical	Lighting
Social	Access	Easiness, Friendly, Prefabricated
		No disparities
		Energy justice
		Vulnerable prioritization
		Inclusion and equity
Art and Cultural	Tradition	Cloud sharing
	Creativity	Sustain traditional aspects
Urban	Building and Infrastructure	Stimulate ecological growth and inclusiveness
		Positive energy needs variation
	Surroundings	Improvement indoor environment
		No rebound or neighborhood effects
	Cities	Minimized environmental conditions effects
Regional/National/Global	Countries/Cross and Beyond	Sustainable and resilient urban climate effects
		Integration with nature-based solutions
		Positive cross-border and boundary effects
		Sustainability&SDG7
		Mitigation of climate change

3.2. Performance Evaluation of Current BIPV Technologies

3.2.1. Opaque (Roof/Facade)

The integration of PV technologies in buildings is constantly increasing. By gaining better insight through concentrated efforts, a variety of innovative solutions to both fundamental pillars of climate neutrality will be promoted. The potential of electricity generated under prominent constraints of technical, environmental, social, and economic issues of the design variables can be estimated with the efficiency improvement towards the reduction in the energy demands. The resulting solutions span from the typical PV added, rooftop, facade, and textures systems to the envelope and glazing integrated components, obviously influenced by the buildings regulations related to performance, such as the EN standards, IEC norms, EBCP directives, or UL standards. They also take into account the mechanical, thermal, and structural properties; fire and noise protection; as well as environmental and climate parameters. The multifunctional elements, as well as integrated devices, address a pronounced and challenging region of improvements from the inputs consideration to the output yield, continuously enriching the lifecycle cost analysis of the process [15].

Radiative heat waves affect electricity generation, as well as the heating and cooling loads of the building and temperature dependents. The facade or rooftop PV excess heat is released to the urban environment, with different diurnal or nocturnal and seasonal behavior. The three expressions of radiation, namely the direct, the diffuse, and the reflected; the short and long wave emissivity of the structural elements of the building and the front and back side PV array surfaces; the local climate conditions; the heat transfer by convection; and reduction by condensation/evaporation are some of the parameters to

consider in order to design environmental optimization between performance and internal comfort. In this context, the thermal performance influence of a building-integrated RTPV system can vary depending on the location, design, and orientation of the building and the PV system, as well as the specific climate conditions [5].

3.2.2. (S)TPV (Glazings)

Semi-transparent PV glazings are a new technology that combine the advantages of regular solar panels with the convenience of windows. These glazings can increase building energy efficiency, lower greenhouse gas emissions, and offer an aesthetically beautiful alternative to traditional solar modules. Three major categories can be used to assess these glazings' performance: thermal, optical, and environmental [23].

The thermal performance of semi-transparent PV glass can be assessed by measuring the U-value, which represents the heat transfer rate through the glazing. Lower U-values indicate improved insulation and reduced heat transfer rates. Furthermore, the solar heat gain coefficient (SHGC) can be measured to determine how much solar radiation the glazing absorbs, affecting the building's heating and cooling loads. Finally, the glass's shading coefficient (SC) can be measured to assess the glazing's ability to block solar radiation.

The optical performance of semi-transparent PV glazing can be assessed by measuring its visible light transmittance (VLT) and reflectance. VLT is the amount of visible light that can flow through the glass, whereas reflectance is the amount of light that is reflected back. The glazing's color, texture, and look can also be assessed to ensure they match aesthetic criteria.

The environmental performance of semi-transparent PV glazing can be assessed by analyzing its durability and resilience to external conditions such as temperature, humidity, and UV radiation. The ability of the glazing to endure wind loads and impact resistance can also be assessed. Furthermore, the environmental impact of the glazing, such as embodied energy, recyclability, and end-of-life disposal, should be considered.

Assessing semi-transparent PV windows' thermal, optical, and environmental performance is crucial to ensure their successful and long-term use in buildings.

4. NZEB Performance

In the model building with the RTPV installation, the simulation results indicated an overall energy demand of 539 MWh or 108 kWh/m² annually, almost twice that of a passive low-energy building. Figure 4 presents a visual representation of how energy demands (heating, cooling, lighting, equipment) fluctuate throughout the year. Notably, the highest demand corresponds to equipment due to the increased power density during the operation of the office building. It remains relatively consistent throughout the year, suggesting a steady energy requirement for powering appliances and machinery. Lighting energy demand exhibits a gradual increase from the darker months to the brighter months, reflecting the influence of daylight availability on energy consumption for lighting purposes. It exceeds 20 kWh/m² mainly due to the core of the building, high light power density (fluorescent tubes), and required level of indoor illuminance (500 lx).

On the other hand, demand for heating and cooling remains below 10 kWh/m² annually. Both are provided by means of electrical energy through the use of a heat pump with an assumed coefficient of performance (COP) of 3. In more detail, heating sharply increases during the colder months, peaking in January. The low demand is explained by the increased heating gains (people, equipment), low thermal transmittance of the building envelope, and good airtightness. Conversely, the cooling demand exhibits a contrasting pattern, with its highest value occurring in July. This highlights the need for cooling systems to maintain indoor comfort for a prolonged summer period in accordance with a previous study [24] for the same climate.

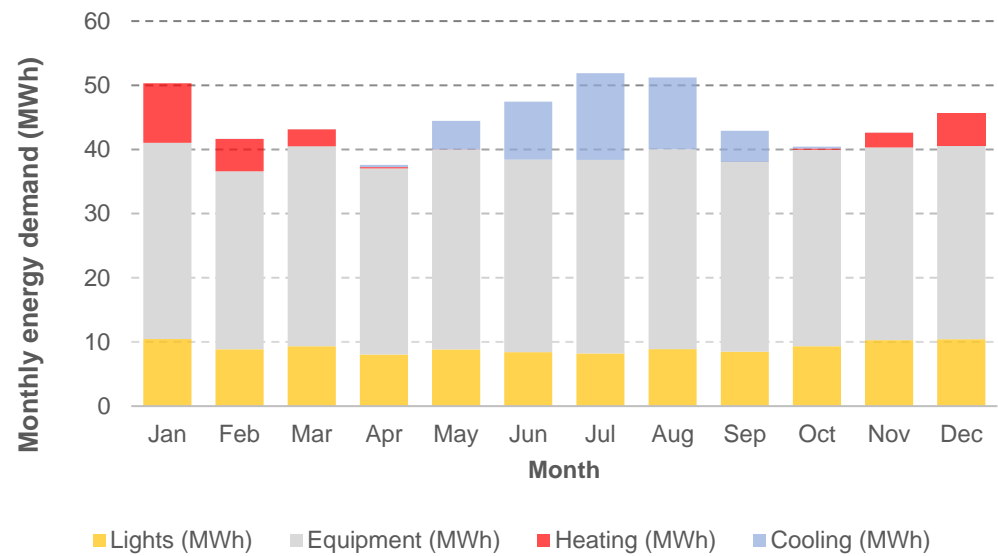


Figure 4. Monthly energy needs for a typical medium-sized office building and semi-continental climate conditions of Prague.

To enhance the roof area effectiveness, as measured by installed capacity per square meter (W/m^2), it was found that a 15 deg tilt angle is the most favorable for balancing self-shading and performance. The simulation results with PV*SOL, depicted in Figure 5, indicate the system's energy production throughout the year. The graph shows that the monthly yield follows a clear seasonal trend. During the summer months, the system achieves its highest yield, as ample sunlight and longer days contribute to increased energy generation. Peak generation occurs in July, corresponding to 21.5 MWh, and coincides with the peak demand. Conversely, the winter months exhibit lower yields, as shorter days and reduced solar radiation limit the system's output. Additionally, the graph reveals certain monthly fluctuations in performance, likely influenced by weather conditions, shading, and maintenance activities.

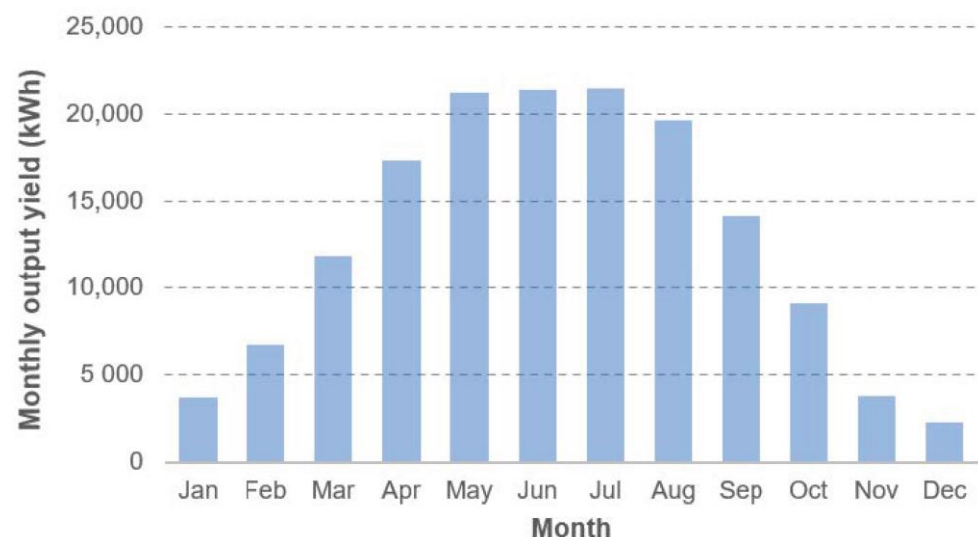


Figure 5. The monthly energy yield of the rooftop PV system and semi-continental climate conditions of Prague.

It was found that the rooftop PV system can generate electricity to cover the annual energy demand by almost 30%. From April until August, the PV yield steadily exceeds 40% of the demand, with the best result in July, where demand is matched by half. Analyzing

these data allow for a comprehensive assessment of the system's energy generation patterns, enabling better optimization strategies, performance monitoring, and informed decision-making regarding the rooftop PV system. Obviously, the building energy performance can be enhanced through the implementation of energy efficiency strategies (e.g., LED lighting) or the selection of a higher PV cover ratio. However, the results clearly indicate the necessity of additional energy sources to achieve a zero energy target in accordance with real monitored data [25] for similar buildings (fully electrified) and climatic conditions. In this direction, the need for PV modules with increased efficiency has become increasingly crucial. By harnessing more energy from each module, higher-efficiency PVs can boost overall system performance, reduce installation costs, and accelerate the adoption of renewable energy in the building sector.

5. Emerging BIPV Technologies

5.1. Opaque

5.1.1. HJT and Modules to Be Produced with Efficiency of up to 25% until 2025

In the past decades, photovoltaic manufacturing processes have shown exceptional advancement by attaining high-efficiency PV values, low degradation rates, and prolonging their lifetime. However, the growth requirements at the TW scale introduce new challenges that need to be deeply addressed in the short term to accelerate the energy transition to a beyond-growth and sustainable future. Moreover, the currently deployed p-type Si modules have reached standard efficiencies of 22%, which is expected to be slightly increased for single-junction silicon modules [26]. The necessity of higher efficiencies at smaller PV dimensions intensified the research efforts, and the more sophisticated heterojunction technology (HJT) solar cells were fabricated to provide higher module efficiencies than conventional cells. These are expected to be widely available in the upcoming years with up to 25% efficiency. Developed by Japanese manufacturers in the 1970s, the patent of HJT was first filed in 1997 by Sanyo. However, after its expiration in 2010, many groups worldwide started to investigate the novel cell architecture towards improving cell performance with less light-induced degradation and elevated temperature degradation. In the typical HJT cell architecture, two a-Si layers with thickness in the nm range are deposited on the front and back sides of a c-Si wafer, one intrinsic and one doped. The former passivates the c-Si while the latter creates the p-n structure with a wide-bandgap from a-Si and a low-bandgap of c-Si to absorb a wider part of the solar spectrum and harvest more energy compared to conventional Si solar cells. In this way, the solar cells' efficiency is increased to higher values than the currently available Si solar cells. An anti-reflective layer (on the front) and transparent conducting oxides (as indium-doped tin oxide) are coated on the front and rear surfaces of the cell to increase light trapping and improve current conduction to the grid electrodes.

The power conversion efficiency of HJT solar cells was expected to reach 24% in 2030 [27]. However, critical technological improvements in the efficiency of solar cells or cost reduction are usually moving faster in implementation than predicted due to the necessity of energy transition. For example, the learning rate of 23% cost reduction for doubling the capacity increased to 40% after 2007 due to the supply chain standardization of solar modules [27]. Therefore, the industry accelerated research in the relative preparation processes, and HJT solar cells with efficiencies of 26.81% were recently achieved by electrically optimized nanocrystalline-silicon hole contact layers [28]. The higher efficiencies are due to the better defect passivation of p-type or n-type Si wafers with hydrogenated nanocrystalline silicon and intrinsic/doped amorphous Si layer depositions on Si wafers, as well as higher carrier mobility in the contact layers (Figure 6). Moreover, the research field of HJT structure is very active with the aim of finding the most suitable carrier-selection contacts to design, optimize, and fabricate novel HJT solar cells with high power conversion efficiencies.

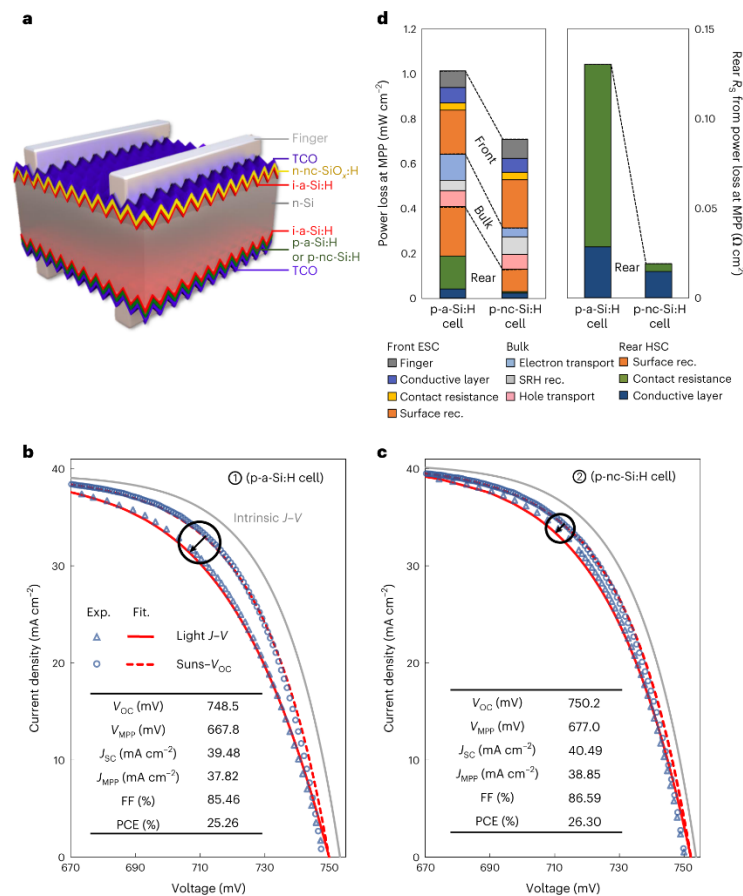


Figure 6. (a) Heterojunction architecture of LONGi solar cell with printed silver grid electrodes and a PCE of 26.81%; (b) J–V curve for a p-a-Si:H cell; (c) J–V curve for a p-nc-Si:H cell (insets: certified cells parameters); (d) power loss and R_S at the maximum power point (MPP) from fitted J–V curves in b and c. In the HJT, n- or p-type doped hydrogenated amorphous silicon (n-a-Si:H or p-a-Si:H) with matched transparent conducting oxides (TCO prepared from 1 wt% CeO_2 doped In_2O_3) are used as electron or hole selection layers in the front and back contact of n-type Czochralski wafers while the intrinsic hydrogenated amorphous silicon (i-a-Si:H) layer enhances the passivation and minimizes the deficit in V_{oc} . Since amorphous silicon is rich in defects, the hydrogenation of nanocrystalline silicon (nc-Si:H) is used to facilitate carrier mobility in n- or p-type doped nc-Si:H. MgF_2 films evaporate on the front and rear TCO layers to further improve current density [28].

In market technology uptake and commercialization, HJT PV bifacial n-type modules with a cell thickness of less than 150 μm , power of panels output 600–700 W, and average PCE efficiency up to 24% are expected to be available soon for residential applications and reach 25% at 2025. Their lifetime is expected to be prolonged compared to the first deployed RTPVs of silicon, with a degradation of around 1.0% in the first year and a power output of approximately 90% of the nominal power output within 30 years. Additional benefits from the industrialization of HJT solar cells are lower production and materials costs due to the low thickness of thin films and shorter and fewer fabrication steps. Therefore, a significant market share of HJT is expected.

5.1.2. Other Emerging Technologies

The dominant concept of the currently applied technologies is based on silicon solar cells under several technologies. The most common wafer-based products are the monocrystalline and polycrystalline solar cells, while the amorphous thin films are un-crystallized silicon films deposited on a substrate. Furthermore, thin film products include non-silicon solar cells, such as gallium arsenide (GaAs), cadmium telluride (CdTe), copper indium dis-

elenide (CIS), and copper indium gallium selenide (CIGS). The efficiencies range up to 14%, 18%, and 20%, respectively, in the thin films, the polycrystalline, and monocrystalline cells, corresponding to different economic performances, yet also sensitive in various design intrinsic and extrinsic parameters of the structure.

Emerging technologies are coming to increase the current efficiency status approaching the Shockley-Queisser (S-Q) limit. The pioneering work on dye-sensitized solar cells (DSSCs) [29], where visible light was converted into electricity through spectral sensitization of wide bandgap dyes, and improvement of the absorption and injection of electrons into the conduction band opened new ways in the era of higher efficiencies potential, low cost, and simple assembly production technology. Since then, many sensitizers have been designed to broaden the wavelength of light harvesting and the charge transfer efficiency.

Besides efficient metal-organic complexes, perovskites were also originally used as dye sensitizers. They rapidly developed due to advantages such as high electron and hole mobility, bandgap tunability, long carrier diffusion length, and low exciton binding energy. The architecture of the device later evolved to planar structures with the perovskite material sandwiched between electron- and hole-transporting layers. In terms of efficiency, the use of mixed solvents to optimize the layers, the combination of low-temperature processing steps, and the control of humidity are some of the strategies to achieve the current certified efficiency above 25% [30]. Due to the undesired thermalization loss in excess of the energy gap or sub-gap regions, many concepts have been proposed to optimize the tradeoff between the photon harvesting maximization and the heat loss minimization, such as multijunction, hot carriers, exciton generated, intermediate bandgap and spectral oriented optimization solar cells [31]. However, only the multijunction solar cells seem to have succeeded [32] in providing viable and promising emerging technologies to meet the increased demands in the field.

The tandem design architecture consists of layered sub-cells connected in series that are selected to manage the induced photocurrent and match the maximum power point output. The alternative configurations have to manage their difficulty in the fabrication processes to succeed in the tradeoff between the technical and economic optimization of the integrated device. The maximum photon harvesting and the minimization of heat losses derived from the excess bandgap or sub-bandgap undesirable thermalization drive the efforts toward enhanced photon-to-charge conversion. Among several other approaches, the multijunction concept, in recent years, demonstrates a better pace in increasing efficiency rate by combining higher open circuit voltage and a broader spectrum of light utilization, and promising to overcome the S-Q limits [33]. The high-quality layers associated with advanced manufacturing technologies multiply the fabrication costs and upscaling processes.

The fabrication of cascaded bandgap perovskite designs with the elimination of the electron transport layer (ETL) saves about one-third of the manufacturing costs leading to further competing costs and time issues. The instability found in most tested configurations is in the infant stage, and efforts are being made to solve the two main problems caused by the direction of material and the transparent conductive oxide (TCO): mismatched energy alignment and ohmic contacts with other layers. The former increases the energy barriers for electron transport and reduces the hole blocking, thus, making the charge transfer and the extraction vulnerable to recombination effects. The latter may act as a shunt to cause current leakage. The gradient homojunction perovskite special design and synthesis by the large cation-assisted method showed fast exciton dissociation and collection, suppressing the recombination of the electrons and holes. The cascaded bandgap design resulted in gradient energy level distribution alignment in the conduction and valence band, enhancing the electron conductivity along the Indium Tin Oxide (ITO) direction and blocking the hole transmission [34].

The commercial implementation of advanced photoconversion efficiencies (PCEs) competes with the existing large-scale production processes due to a considerable advantage in the marketplace. Still, most of the time, the former requires an increased levelized energy

cost, making them appropriate to specific applications where the power density is essential, e.g., due to space confinement, such as in RTPVs, facade, or building envelope applications.

The experience gained from the silicon-based solutions is important and contributes to the knowledge transfer to new technologies' perspectives, ranging from the degradation phenomena to the lifetime assessment [26]. PV degradation is an important issue in the current PV technologies. Research efforts are concentrated on more accurate diagnosis and testing methods, improved understanding of its causes, development of new materials and techniques for preventing PV degradation, long-term testing and performance evaluation for PV hotspots and cracks prevention, and the standardization of testing methods [35].

Integrating new PSCs technologies with other PV cells to form tandem solar cells with a high-performance ratio creates a competitive advantage towards leveraging the existing technologies. The enhanced efficiency leads to the economic viability of the minimum acceptable manufacturing costs [36]. Several strategies are employed to investigate the required high PCE, the long-term stability, and the fast response characteristics, which, eventually, the improvement of one of which will come at the expense of the other [37]. The synergistic effect of additive engineering to improve the PSCs' performance focuses on the crucial issues associated with the density defect and surface passivation by partially placing more stable metals instead conventional Pb, but this affects the required low band, the carrier lifetime, and the diffusion length and increase in recombination losses [38]. The tunability of energy bandgaps, the transmittance control of incident light at the top cell, the high conductivity, and the transparency optical properties of carbon electrodes with hydrophobic properties seem to be an ideal solution for high performance and, beside the elimination of the hole transfer layer, the lowering the of fabrication costs and metal-free solutions are in infant stage [39].

Since the electricity output efficiency is of the utmost importance for the life cycle assessment of the module, it affects both the production factors productivity and the cumulative market price learning curve in a downslope fashion through demand increase. The challenging tasks, from innovative lab solutions to fab sustainable upscaling processes, include systematic research in resource properties, optimization of manufacturing technologies, and commercialization of viable prices [36].

Stability is critical to BIPV technologies as they need to withstand long-term exposure to various environmental conditions. However, one major challenge associated with perovskite materials is their stability and reliability over time. Perovskite solar cells can degrade under various environmental conditions, including moisture, heat, light, and oxygen exposure [40,41]. Additionally, inherent properties of perovskite materials, such as ion migration and low defect formation energy, contribute to the rapid degradation of perovskite films [42]. Meeting the market requirement of a 25-year outdoor operational lifetime remains a hurdle for PSCs. Several strategies are being explored to enhance their resistance to degradation, ensuring their longevity in building applications.

One effective approach is to adjust the composition of perovskite materials by incorporating different elements or dopants to improve their stability. For example, replacing the volatile methylammonium (MA) cation with more stable formamidinium (FA), cesium (Cs) [43], and rubidium (Rb) [44]. Secondly, passivation methods such as using small organic molecules or polymers to passivate surface or bulk defects have improved stability. For example, employing fullerene derivatives [45] or incorporating polymers [46] into the perovskite film can help mitigate defects and enhance stability. Designing novel device architectures, such as multilayer or tandem structures, can enhance stability. For instance, forming multidimensional perovskite structures, like 2D/3D configurations, can suppress the migration of ionic species and improve stability [47]. Thirdly, inorganic candidates such as NiOx, CuOx, and CuSCN are introduced as substitutes for organic materials, particularly for the hole-transporting layer (HTL) [48–50]. Finally, it is worth noting that encapsulating PSCs, as with other PV technologies, can extend their lifetime by protecting them against external environmental factors [51].

5.1.3. Glazings

Unlike opaque solar cells, semi-transparent photovoltaics (STPVs) have the potential for novel applications that combine solar energy harvesting and light transmission. STPV solar cells are up-and-coming candidates for building integration via glazing, skylight, or other building envelope applications. The main challenge is achieving adequate average visible transmittance (AVT) and high-power conversion efficiency (PCE) [52]. The theoretical Shockley–Queisser (SQ) limit for a single-junction wavelength-selective transparent solar cell with a 100% AVT is around 20.6%, but this is yet to be achieved [53]. Emerging technologies, such as perovskite, dye-sensitized, and organic PV, are expected to enter the market, driving down costs and expanding the range of available products [54,55].

Organic solar cells (OPVs) offer significant advantages over traditional silicon cells, making them well-suited for STPVs. These advantages include lower manufacturing costs, optimized photoactive layer thickness, the capability to be printed on flexible substrates, and adjustable optical properties [56]. Organic polymers and small molecules in OPV cells absorb light and convert it to electricity. Recent advancements in materials science and device engineering have resulted in semi-transparent OPVs with efficiencies exceeding 10%. We report an OPV device by Liu et al. [57] with an AVT = 46.79% and a PCE = 11.44%. The cell's transparent rear electrode was designed with an aperiodic band-pass filter made of [lithium fluoride [LiF]/tellurium dioxide[TeO₂]]₈/LiF produced by thermal evaporation. Jing et al. [58] described a method for improving the optical and electrical performance of ST-OPV by using 2PACz additive as a replacement for PEDOT:PSS. As a result, the PCE was 15.2%, with an AVT of 19.2%. Increasing the AVT to 30% kept the PCE at 11.3%. Overall, developing high-efficiency semi-transparent OPVs is an active area of research, and it is anticipated that advancements in materials science and device engineering will further their performance and commercial viability. So far, several companies are currently working on developing OPV glass products, such as Heliatek and Armor solar power films.

Another promising technology for BIPV applications is semi-transparent DSSC modules. DSSCs are thin-film solar cells that absorb light and generate electrical current using organic dyes [29]. They have several advantages over traditional silicon solar cells, including lower manufacturing costs [59], greater flexibility and transparency, and a positive temperature coefficient [60]. Several studies have shown that semi-transparent DSSC modules for BIPV applications are feasible, with their power conversion efficiencies ranging from 4% to 8% [61]. However, their long-term stability and durability must be addressed to ensure commercial viability. Several companies are currently working on developing DSSC glass products, such as Solaronix and G24 Power.

PSCs are the most promising ST solar cell candidates among the currently available solar cells. Perovskite solar cells have advanced rapidly in the last decade, with excellent optical properties and power conversion efficiency (PCE) exceeding 25%. Several studies have looked into semi-transparent perovskite cells for BIPV applications, proving their feasibility and potential for high power output [62]. PCEs of 8–12% are currently achievable with semi-transparent PSCs with AVTs ranging between 20 and 30%. For example, Yu et al. [63] created a semi-transparent cell with AVT = 35% and PCE = 12%. Their optimization strategy was based on fine-tuning the cesium (Cs) and formamidinium (FA) perovskite composition, which they believe will produce the best device performance across a wide range of bandgaps. Several companies are currently working on developing perovskite PV glass products, including Oxford PV, Saule Technologies, and Swift Solar. Problems such as long-term stability and durability must be solved to ensure commercial viability.

Luminescent solar concentrators (LSCs) can ultimately transform how we generate solar energy from windows. LSCs are essentially transparent plates or sheets coated with a luminescent material that absorbs and re-emits sunlight at longer wavelengths. This re-emitted light is then directed to the plate's edges, where solar cells convert the light into electricity [64]. This technology provides several benefits for window-integrated photovoltaics, including low-cost manufacturing, flexibility, and the ability to capture light from all angles, making them especially well-suited for urban environments [65]. Several

research groups have shown that LSCs for BIPV applications are feasible, with power conversion efficiencies ranging from 2% to 8% [66,67].

6. Tandem Cells with Efficiencies of up to 30%

PV cells in the market typically have a maximum efficiency of 20–25%, approaching the theoretical limit (29.4%) of single junction silicon (c-Si) cells. In order to enhance efficiency further, researchers are actively exploring innovative approaches such as multijunction or tandem solar cells (TSCs). Tandem solar cells are photovoltaic (PV) devices comprising multiple photovoltaic absorbers with varying energy bandgaps. This arrangement allows for more effective solar spectrum utilization, as these cells absorb a fraction of incident photons with energies higher than the wide-bandgap absorber (Figure 7). Meanwhile, lower-energy photons pass through to the bottom subcell, where the low-band-gap active layer harvests them. Tandem solar cell efficiency is being improved through ongoing research and development, and efficiency is expected to rise further in the coming years. Devices utilizing two-terminal (2T) or four-terminal (4T) architecture have already achieved efficiencies exceeding 30% [30], surpassing the single-junction solar cell limit [68].

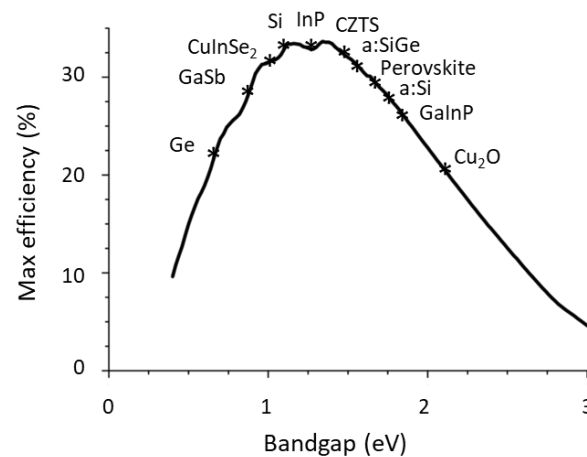


Figure 7. Bandgaps of potential or/and tested top cells in hybrid tandem solar cells with c-Si as the bottom cell in the theoretical curve of the maximum single p-n junction cell efficiency of the Shockley–Queisser limit.

Perovskite solar cells (PSCs) have emerged as promising candidates for tandem photovoltaics because of their high power-conversion efficiency and tunable bandgap. Integrating a wide-bandgap perovskite with well-established low-bandgap materials such as Si to build tandem solar cells has attracted considerable attention from the scientific community and industry stakeholders since their initial reports in 2015 [69]. Through persistent and focused research endeavors, silicon/perovskite TSCs have recently achieved 32.5% certified efficiency [30]. An up-to-date chronological development of tandem solar cells according to the material used and their certified efficiencies is presented in Figure 8.

The two-terminal (2T) perovskite/Si TSC, where the perovskite top cell is directly fabricated on the Si bottom cell, is preferred for easier fabrication and reduced cost. Köhnen et al. [70] demonstrated industrially relevant (industry-compatible bottom cells) perovskite/Si tandem solar cells with 27.9% efficiency based on thin (<200 μm thick) Czochralski silicon bottom cells. In the three- or four-terminal (3T or 4T) configurations, the perovskite and Si cells are fabricated separately, making them electrically independent.

On the other hand, using perovskite solar cells for tandem applications presents several challenges, including issues with stability, reliability, and the need for efficient and reliable interconnects between the two cells [71]. In this regard, research has focused on strategies for optimizing the perovskite material [72], designing appropriate interlayers [73], and exploring new device architectures. Further advancement to resolve challenges related to PSC stability [74] and justify 25-year warranties and scalable fabrication [75] is critical to

bridge the gap in the commercial readiness of this technology, which is also undergoing extensive investigation. Exploring scalable manufacturing processes for emerging BIPV technologies, including roll-to-roll printing and solution-based [76] or vacuum-based deposition methods [77], can streamline production and reduce manufacturing costs. By addressing these challenges in recent years, the perovskite/silicon tandem roadmap can be extended beyond 30% efficiency [78].

The implementation of emerging technologies in real-world settings encounters obstacles associated with light and temperature-induced degradation. Despite these challenges, certain Perovskite/Si tandem cells have exhibited impressive power output, retaining 80% of their initial capacity even after enduring a year of exposure to severe weather conditions [79]. In addition, scalable fabrication of tandems on industrially textured silicon demonstrated an efficiency of 25.1% for an aperture area of 16 cm² [80]. These specific findings represent a significant step towards the commercialization of tandem photovoltaics, and showcase the potential for improved efficiency and viability in real-world applications. According to the International Technology Roadmap for Photovoltaics (ITRPV) report [81], Si-based tandems will enter mass production after 2019 and account for 5% of the market within ten years. The Oxford PV company already houses the world's first volume manufacturing line for perovskite-on-silicon tandem, while production is expected within 2023.

On the other hand, the low absorption coefficient and high silicon module cost are significant barriers to the mass production of perovskite/silicon TSCs. As a result, new materials other than Si must be investigated for use as the absorber layer in the bottom cell in PV technology. Despite having a lower reported efficiency, (Figure 8) than silicon, Perovskite/CIGS tandems can be produced on flexible substrates with a lower carbon footprint per kWh produced. Han et al. [82] used nanoscale CIGS surface interface engineering and a heavily doped PTAA hole transport layer between the subcells to preserve open-circuit voltage while increasing the fill factor and short-circuit current. The monolithic perovskite/CIGS tandem solar cell achieved a 22.43% efficiency, and unencapsulated devices maintained 88% of their initial efficiency after 500 h of aging under continuous 1-sun illumination. Removing the degraded perovskite front cell did not harm the CIGS device, and the re-used tandem devices had similar efficiencies. In 2022, Jošt et al. [83] reported on the highest-efficiency monolithic perovskite/CIGS tandem cell with a certified record PCE of 24.2%. Simulation results from the same authors revealed that a PCE of 32% could realistically be achieved by optimizing the device stack.

Notable results in tandem configurations have been achieved by combining perovskite and low bandgap copper indium diselenide (CIS), with impressive 30.2% and 23.4% efficiency [84], as well as perovskite-PbS CQD monolithic tandem by Madan et al. [85] with 23.36% efficiency. Tandems based on thin films have great potential for high-throughput and cost-effective production of flexible and lightweight TSCs and thus are promising for integrated photovoltaics applications. Nejang et al. [86] used scalable fabrication methods to create all-perovskite tandem modules with up to 19.1% conversion efficiencies. He et al. [87] recently used 4PADCB as a hole-selective layer for wide-bandgap perovskite solar cells, demonstrating a 1 cm² all-perovskite tandem with low FF losses and a certified record efficiency of 27%.

Perovskite-organic tandem solar cells (PO-TSCs) are especially interesting among different kinds of tandem cells as they can benefit from the complementary characteristics of organic solar cells (OSCs) and perovskite solar cells (PSCs). PO-TSCs can surpass current tandem solar cells in device performance, manufacturing cost, and potential applications. After the first reports on monolithic Perovskite/organic tandem solar cells, little progress was made until Chen et al. [88] presented the first device that exceeded 20% efficiency. Recently, a new record PCE of 23.21% was reported by Sun et al. [89]. The authors introduced an ionic liquid-based dual-interface engineering strategy for improving the performance of the front wide-bandgap CsPbI₂Br perovskite sub-cells. Combined with the narrow-bandgap PM6:CH1007-based sub-cells, the assembled tandem devices not only had high

PCE but also possessed increased device stability, demonstrating their competitiveness compared to other tandem architectures.

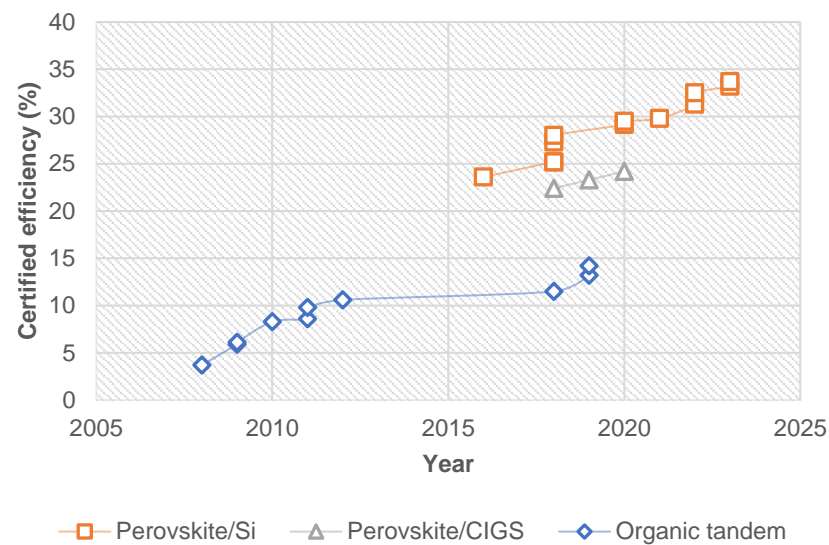


Figure 8. Chronological development of tandem solar cells with certified efficiency (data source: NREL [90]).

New designed 2D tandem PV materials based on III–V and II–VI compounds have also been proposed for high-efficiency active solar energy systems [91]. The efficiency of tandem structures in III–V multi-junction solar cells has reached very high-efficiency levels at the lab scale, and the 30% milestone for BIPV modules can be considered attainable within the upcoming years. However, the cost of these materials remains an order of magnitude higher than for c-Si. At the same time, their elemental earth scarcity would likely become a factor for an upscaled rooftop photovoltaic implementation. Therefore, other candidate materials such as CuInS₂ or Cu₂ZnSnS₄; amorphous silicon; Se; or Cu₂O could be used for the top cell of tandem structures.

Moreover, the industrialization costs of materials and energy flow hold different production factors and technology processes, while the total lifecycle assessment, the capacity factor, and efficiency obtained are taken into consideration.

Even with their promising potential for commercialization, emerging BIPV and tandem devices encounter comparable significant technical challenges, including stability, scalability, and replicability [92]. Efficiency and stability enhancements are sought to offset the additional costs of constructing tandem structures. The main barrier refers to the PSC part of any device, especially due to the expensive layer material. The homojunction p-type wafer-based approach may help reduce the costs and the silicon-based bottom cell. In any way, the research is being directed toward more cost-effective processes, cheaper materials, and feasible techniques.

Nevertheless, they have received limited consideration from a techno-economic perspective, which may influence future research efforts. Under techno-economic analysis, tandem solar cells exhibit a higher levelized cost of energy (LCOE) due to the higher capital expenditures than silicon solar cells. Li et al. [93] investigated the techno-economic competitiveness of four PV modules: mc-silicon, perovskite single junction, perovskite/c-silicon tandem, and perovskite/perovskite tandem. Their results indicated that perovskite PVs exhibit low materials cost, which substantially reduces (up to 21%) the LCOE in both the single-junction and tandem devices. Still, module efficiency and lifetime are the dominant parameters that affect the LCOE significantly.

The improvement of long-term stability of PSCs similar to silicon-based cells is an important factor to compare for in the same period of industrialized costs. Long-term sta-

bility also plays a major role in the life cycle assessment, in addition to zero environmental toxicity and net-zero fabrication operating emissions [77].

However, crucial issues toward the industrialization of tandem cells have started to be resolved, and preliminary results show that devices with a PCE of over 30% and a size of $\sim 64 \text{ cm}^2$ can be realized by a combination of $\sim 19\%$ -PCE semi-transparent perovskite single junction module and a c-Si heterojunction back-contact solar cell [94]. Additionally, the compatibility of tandem photovoltaics with existing infrastructure, such as electrical grids and power distribution systems, is an advantage. Tandem cells can be designed to have similar electrical characteristics to conventional solar cells, allowing for easy integration into the existing energy infrastructure (electrical grids and power distribution systems).

New solar cell development which can surpass the silicon Shockley–Queisser efficiency limit without increasing the cost or the simplifying of the manufacturing process is a major challenge in PV research [95]. However, recent intense research efforts in new tandem concepts, such as perovskite/Si, have led to a substantial advance in the field and have raised the possibility of accelerated commercialization. Compatibility between the tandem subcells is a critical issue and a challenge to optimizing the best subcell interconnection configurations [96]. To this direction, several EU projects were or are being funded on tandem solar cells, such as all-perovskite, perovskite/silicon, or III-V/Si solar cells, with efficiencies expected to reach and even exceed the 30% limit before 2030 alongside being manufactured at low-cost ($<0.4 \text{ EUR/Wp}$) (projects PERTPV, CHEOPS, LOVETandemSolar, HYPERION, SiTaSol, Crystal Tandem Solar, HIPERION, POSITS, Nano-Tandem, S-PSK-PSK-MJ-PSC, MIRACLE with detailed progress available at cordis.europa.eu, last accessed 16 July 2023), eco-designed (e.g., project NEXUS with modules efficiency $>30\%$), and flexible for potential use in BIPV applications. For example, innovative eco-design approaches are considered in the NEXUS project [97] coordinated by the CEA (Commissariat à l'Énergie Atomique et aux Énergies Alternatives) and funded by HORIZON Europe until October 2025, with solvent-free perovskite deposition, circularity, recyclability, and improved, simple manufacturing processes towards a viable economic pathway for the European commercialization of tandem perovskite. In the 4SUNS project [98] funded by the excellent Science—European Research Council (ERC) until September 2026, a 4-colours/2-junctions structure will be grown by a molecular beam epitaxy system, and the final devices will be manufactured as breakthrough competitive products.

With all these efforts, the manufacturing costs of perovskite modules with efficiencies higher than 25% are expected to be of comparable costs to current Si technologies, while the multijunction technology such as tandem III-V/Si solar cells ($>30\%$ module efficiency) or perovskite-silicon tandem devices ($>30\%$ module efficiency) are the two most promising and efficient technologies for pilot lines establishment until 2030 [99].

7. Conclusions

PV growth has been remarkable during the last few years. It is among the most mature technologies to be dispatched quickly for a major contribution to the full decarbonization and elimination of GHGs from fossil fuels. This can be accomplished by electrification, either directly with the use of heat pumps and electric vehicles or indirectly by producing hydrogen or synthetic fuels to substitute fossil fuels. To increase the electricity generation of BIPVs in cities and eliminate any potential overheating effect, high-efficiency or multi-junction solar cells are necessary. Many materials with excellent mechanical and flexible properties, such as perovskites and tandem cells, have been prepared with very high efficiencies ($>25\%$). These cells have been proposed as appropriate for addition to existing building structures or for direct integration as components, thus replacing building construction materials and reducing integration costs. However, integrating emerging BIPV into existing building structures and infrastructure present challenges since modifications may be required to accommodate the installation and connection of these specialized solar modules. Compatibility with electrical grids and existing power distribution systems, including inverters and storage solutions, also needs to be addressed for seamless integration.

Additionally, intense efforts are being directed at minimizing the environmental impact of potential solutions by using toxic-free materials in high-efficiency single or tandem solar cells. Moreover, EU regulations on eco-designed modules and their energy labelling are soon being implemented. Colored photovoltaics or antireflection coatings and dielectric materials as additives offer a variety of different colors to facilitate their architectural integration in the urban environment.

Additive engineering improvements are on the way to accelerate the transition from lab innovations to fabrication at minimum efficient scales. The leverage of existing silicon-based technologies improves the PCE efficiencies, stability issues, and fast response of characteristics for long-term viability.

According to the literature, three years are required to forward the lab average solar cell efficiency to commercial products. Additionally, the size of the cell has increased remarkably during the last two decades to more than 200 mm square wafers. With many champion cells at the lab with an efficiency higher than 30% and an increase in little more than the current 0.5% per year, the industrial milestone of 30% BIPV efficiency in 2030 of eco-designed products with a longer lifetime can be feasibly reached.

Author Contributions: Conceptualization, methodology and original draft preparation, N.S., V.K. and D.K.; Writing—review and editing, N.S., V.K., T.M. and D.K. All authors have read and agreed to the published version of the manuscript.

Funding: This research received no external funding.

Institutional Review Board Statement: Not applicable.

Informed Consent Statement: Not applicable.

Data Availability Statement: Not applicable.

Acknowledgments: N. Skandalos acknowledges support by ERA-NET-SES “Deployment of Smart Renewable Energy Communities” (DoRES) project.

Conflicts of Interest: The authors declare that the research was conducted in the absence of any commercial or financial relationships that could be construed as a potential conflict of interest.

References

1. Santamouris, M. Cooling the cities—A review of reflective and green roof mitigation technologies to fight heat island and improve comfort in urban environments. *Sol. Energy* **2014**, *103*, 682–703. [CrossRef]
2. Cuerdo-Vilches, T.; Díaz, J.; López-Bueno, J.A.; Luna, M.Y.; Navas, M.A.; Mirón, I.J.; Linares, C. Impact of urban heat islands on morbidity and mortality in heat waves: Observational time series analysis of Spain’s five cities. *Sci. Total Environ.* **2023**, *890*, 164412. [CrossRef]
3. Eugenio Pappalardo, S.; Zanetti, C.; Todeschi, V. Mapping urban heat islands and heat-related risk during heat waves from a climate justice perspective: A case study in the municipality of Padua (Italy) for inclusive adaptation policies. *Landsc. Urban Plan.* **2023**, *238*, 104831. [CrossRef]
4. Iungman, T.; Cirach, M.; Marando, F.; Barboza, E.P.; Khomenko, S.; Masselot, P.; Quijal-Zamorano, M.; Mueller, N.; Gasparrini, A.; Urquiza, J. Cooling cities through urban green infrastructure: A health impact assessment of European cities. *Lancet* **2023**, *401*, 577–589. [CrossRef]
5. Skandalos, N.; Wang, M.; Kapsalis, V.; D’Agostino, D.; Parker, D.; Bhuvad, S.S.; Udayraj; Peng, J.; Karamanis, D. Building PV integration according to regional climate conditions: BIPV regional adaptability extending Köppen-Geiger climate classification against urban and climate-related temperature increases. *Renew. Sustain. Energy Rev.* **2022**, *169*, 112950. [CrossRef]
6. International Energy Agency (IEA). Solar PV Technology Deep Dive. Available online: <https://www.iea.org/reports/solar-pv> (accessed on 21 February 2023).
7. Castellanos, S.; Sunter, D.A.; Kammen, D.M. Exploring rooftop solar photovoltaics deployment and energy injustice in the US through a data-driven approach. In *Data Science Applied to Sustainability Analysis*; Elsevier: Amsterdam, The Netherlands, 2021; pp. 109–128.
8. Kammen, D.M.; Sunter, D.A. City-integrated renewable energy for urban sustainability. *Science* **2016**, *352*, 922–928. [CrossRef] [PubMed]
9. Romani, J.; Pérez-Rodríguez, A.; Salom, J. Performance of prototype tandem UV filter and organic transparent photovoltaic windows. *J. Build. Eng.* **2023**, *68*, 106111. [CrossRef]

10. Tian, X.; Wang, J.; Ji, J.; Wang, C.; Ke, W.; Yuan, S. A multifunctional curved CIGS photovoltaic/thermal roof system: A numerical and experimental investigation. *Energy* **2023**, *273*, 127259. [CrossRef]
11. Koh, T.M.; Wang, H.; Ng, Y.F.; Bruno, A.; Mhaisalkar, S.; Mathews, N. Halide perovskite solar cells for building integrated photovoltaics: Transforming building façades into power generators. *Adv. Mater.* **2022**, *34*, 2104661. [CrossRef]
12. Nguyen, D.C.; Sato, K.; Hamada, M.; Murata, F.; Ishikawa, Y. Annual output energy harvested by building-integrated photovoltaics based on the optimized structure of 2-terminal perovskite/silicon tandem cells under realistic conditions. *Sol. Energy* **2022**, *241*, 452–459. [CrossRef]
13. D’Agostino, D.; Parker, D.; Melià, P.; Dotelli, G. Optimizing photovoltaic electric generation and roof insulation in existing residential buildings. *Energy Build.* **2022**, *255*, 111652. [CrossRef]
14. Garshasbi, S.; Khan, A.; Santamouris, M. On the building cooling energy penalty of photovoltaic solar panels in Sydney. *Energy Build.* **2023**, *294*, 113259. [CrossRef]
15. Jelle, B.P.; Breivik, C.; Drolsum Røkenes, H. Building integrated photovoltaic products: A state-of-the-art review and future research opportunities. *Sol. Energy Mater. Sol. Cells* **2012**, *100*, 69–96. [CrossRef]
16. Pillai, D.S.; Shabunko, V.; Krishna, A. A comprehensive review on building integrated photovoltaic systems: Emphasis to technological advancements, outdoor testing, and predictive maintenance. *Renew. Sustain. Energy Rev.* **2022**, *156*, 111946. [CrossRef]
17. Polverini, D.; Amillo, A.G.; Taylor, N.; Sample, T.; Salis, E.; Dunlop, E.D. Building Criteria for Energy Labeling of Photovoltaic Modules and Small Systems. *Sol. RRL* **2022**, *6*, 2100518. [CrossRef]
18. Wade, A.; Neuhaus, H.; Probst, L.; Sauer, T.; Moser, D.; Rohr, C.; Rossi, R.; Wirth, H. *Expert Input Paper-Eco-Design & Energy Labelling for Photovoltaic Modules, Inverters and Systems in the EU*; Secretariat of the European Technology and Innovation Platform for Photovoltaics: Brussels, Belgium, 2021. [CrossRef]
19. Ecodesign-European Commission to Examine New Rules on Environmental Impact of Photovoltaics. Available online: <https://ec.europa.eu> (accessed on 11 July 2023).
20. Commission, E. Regulation (EU) No 305/2011 of the European Parliament and of the Council of 9 March 2011 laying down harmonized conditions for the marketing of construction products and repealing Council Directive 89/106/EEC. *Off. J. Eur. Union* **2011**, *88*, 5–43.
21. ICARES; CSTB; SUPSI; TECNALIA; TULiPPS. Regulatory Framework for BIPV, Report of Project BIPVboost; 2019. Report of the Horizon Project BIPV Boost. Available online: <https://bipvboost.eu/public-reports/?page=2> (accessed on 6 July 2023).
22. Haegel, N.M.; Verlinden, P.; Victoria, M.; Altermatt, P.; Atwater, H.; Barnes, T.; Breyer, C.; Case, C.; De Wolf, S.; Deline, C. Photovoltaics at multi-terawatt scale: Waiting is not an option. *Science* **2023**, *380*, 39–42. [CrossRef]
23. Skandalos, N.; Karamanis, D. PV glazing technologies. *Renew. Sustain. Energy Rev.* **2015**, *49*, 306–322. [CrossRef]
24. Skandalos, N.; Tywoniak, J. Influence of PV facade configuration on the energy demand and visual comfort in office buildings. *J. Phys. Conf. Ser.* **2019**, *1343*, 012094. [CrossRef]
25. Skandalos, N.; Kichou, S.; Wolf, P. Energy sufficiency of an administrative building based on real data from one year of operation. In Proceedings of the 2018 Smart City Symposium Prague (SCSP), Prague, Czech Republic, 24–25 May 2018; pp. 1–8.
26. Ballif, C.; Haug, F.-J.; Boccard, M.; Verlinden, P.J.; Hahn, G. Status and perspectives of crystalline silicon photovoltaics in research and industry. *Nat. Rev. Mater.* **2022**, *7*, 597–616. [CrossRef]
27. Victoria, M.; Haegel, N.; Peters, I.M.; Sinton, R.; Jäger-Waldau, A.; del Canizo, C.; Breyer, C.; Stocks, M.; Blakers, A.; Kaizuka, I. Solar photovoltaics is ready to power a sustainable future. *Joule* **2021**, *5*, 1041–1056. [CrossRef]
28. Lin, H.; Yang, M.; Ru, X.; Wang, G.; Yin, S.; Peng, F.; Hong, C.; Qu, M.; Lu, J.; Fang, L. Silicon heterojunction solar cells with up to 26.81% efficiency achieved by electrically optimized nanocrystalline-silicon hole contact layers. *Nat. Energy* **2023**, 1–11. [CrossRef]
29. O’regan, B.; Grätzel, M. A low-cost, high-efficiency solar cell based on dye-sensitized colloidal TiO₂ films. *Nature* **1991**, *353*, 737–740. [CrossRef]
30. Photovoltaic Research | NREL, “Best Research-Cell Efficiency Chart”. Available online: <https://www.nrel.gov/pv/cell-efficiency.html> (accessed on 1 June 2023).
31. Kapsalis, V.; Kyriakopoulos, G.; Zamparas, M.; Tolis, A. Investigation of the photon to charge conversion and its implication on photovoltaic cell efficient operation. *Energies* **2021**, *14*, 3022. [CrossRef]
32. Wang, Z.; Song, Z.; Yan, Y.; Liu, S.; Yang, D. Perovskite—A perfect top cell for tandem devices to break the S–Q limit. *Adv. Sci.* **2019**, *6*, 1801704. [CrossRef]
33. Rühle, S. Tabulated values of the Shockley–Queisser limit for single junction solar cells. *Sol. Energy* **2016**, *130*, 139–147. [CrossRef]
34. Gao, L.; Xu, C.; Su, Y.; Liu, A.; Ma, T. Cascaded band gap design for highly efficient electron transport layer-free perovskite solar cells. *Chem. Commun.* **2022**, *58*, 6749–6752. [CrossRef] [PubMed]
35. Badran, G.; Dhimish, M. Potential Induced Degradation in Photovoltaic Modules: A Review of the Latest Research and Developments. *Solar* **2023**, *3*, 322–346. [CrossRef]
36. Song, Z.; McElvany, C.L.; Phillips, A.B.; Celik, I.; Krantz, P.W.; Watthage, S.C.; Liyanage, G.K.; Apul, D.; Heben, M.J. A technoeconomic analysis of perovskite solar module manufacturing with low-cost materials and techniques. *Energy Environ. Sci.* **2017**, *10*, 1297–1305. [CrossRef]
37. Li, T.T.; Yang, Y.B.; Li, G.R.; Chen, P.; Gao, X.P. Two-Terminal Perovskite-Based Tandem Solar Cells for Energy Conversion and Storage. *Small* **2021**, *17*, 2006145. [CrossRef]

38. Kim, D.H.; Muzzillo, C.P.; Tong, J.; Palmstrom, A.F.; Larson, B.W.; Choi, C.; Harvey, S.P.; Glynn, S.; Whitaker, J.B.; Zhang, F. Bimolecular additives improve wide-band-gap perovskites for efficient tandem solar cells with CIGS. *Joule* **2019**, *3*, 1734–1745. [[CrossRef](#)]
39. Hwang, S.K.; Park, I.J.; Seo, S.W.; Park, J.H.; Park, S.J.; Kim, J.Y. Electrochemically deposited CZTSSe thin films for monolithic perovskite tandem solar cells with efficiencies over 17%. *Energy Environ. Mater.* **2023**, e12489. [[CrossRef](#)]
40. Salhi, B.; Wudil, Y.; Hossain, M.; Al-Ahmed, A.; Al-Sulaiman, F. Review of recent developments and persistent challenges in stability of perovskite solar cells. *Renew. Sustain. Energy Rev.* **2018**, *90*, 210–222. [[CrossRef](#)]
41. Djurišić, A.; Liu, F.; Ng, A.M.; Dong, Q.; Wong, M.K.; Ng, A.; Surya, C. Stability issues of the next generation solar cells. *Phys. Status Solidi (RRL)–Rapid Res. Lett.* **2016**, *10*, 281–299. [[CrossRef](#)]
42. Bati, A.S.; Zhong, Y.L.; Burn, P.L.; Nazeeruddin, M.K.; Shaw, P.E.; Batmunkh, M. Next-generation applications for integrated perovskite solar cells. *Commun. Mater.* **2023**, *4*, 2. [[CrossRef](#)]
43. Saliba, M.; Matsui, T.; Seo, J.-Y.; Domanski, K.; Correa-Baena, J.-P.; Nazeeruddin, M.K.; Zakeeruddin, S.M.; Tress, W.; Abate, A.; Hagfeldt, A. Cesium-containing triple cation perovskite solar cells: Improved stability, reproducibility and high efficiency. *Energy Environ. Sci.* **2016**, *9*, 1989–1997. [[CrossRef](#)]
44. Syzgantseva, O.A.; Saliba, M.; Grätzel, M.; Rothlisberger, U. Stabilization of the perovskite phase of formamidinium lead triiodide by methylammonium, Cs, and/or Rb doping. *J. Phys. Chem. Lett.* **2017**, *8*, 1191–1196. [[CrossRef](#)]
45. Deng, L.L.; Xie, S.Y.; Gao, F. Fullerene-Based Materials for Photovoltaic Applications: Toward Efficient, Hysteresis-Free, and Stable Perovskite Solar Cells. *Adv. Electron. Mater.* **2018**, *4*, 1700435. [[CrossRef](#)]
46. Wang, S.; Zhang, Z.; Tang, Z.; Su, C.; Huang, W.; Li, Y.; Xing, G. Polymer strategies for high-efficiency and stable perovskite solar cells. *Nano Energy* **2021**, *82*, 105712. [[CrossRef](#)]
47. Proppe, A.H.; Johnston, A.; Teale, S.; Mahata, A.; Quintero-Bermudez, R.; Jung, E.H.; Grater, L.; Cui, T.; Filleter, T.; Kim, C.-Y. Multication perovskite 2D/3D interfaces form via progressive dimensional reduction. *Nat. Commun.* **2021**, *12*, 3472. [[CrossRef](#)]
48. You, J.; Meng, L.; Song, T.-B.; Guo, T.-F.; Yang, Y.; Chang, W.-H.; Hong, Z.; Chen, H.; Zhou, H.; Chen, Q. Improved air stability of perovskite solar cells via solution-processed metal oxide transport layers. *Nat. Nanotechnol.* **2016**, *11*, 75–81. [[CrossRef](#)]
49. Sun, W.; Li, Y.; Ye, S.; Rao, H.; Yan, W.; Peng, H.; Li, Y.; Liu, Z.; Wang, S.; Chen, Z. High-performance inverted planar heterojunction perovskite solar cells based on a solution-processed CuO x hole transport layer. *Nanoscale* **2016**, *8*, 10806–10813. [[CrossRef](#)] [[PubMed](#)]
50. Ye, S.; Sun, W.; Li, Y.; Yan, W.; Peng, H.; Bian, Z.; Liu, Z.; Huang, C. CuSCN-based inverted planar perovskite solar cell with an average PCE of 15.6%. *Nano Lett.* **2015**, *15*, 3723–3728. [[CrossRef](#)] [[PubMed](#)]
51. Matteocci, F.; Cinà, L.; Lamanna, E.; Cacovich, S.; Divitini, G.; Midgley, P.A.; Ducati, C.; Di Carlo, A. Encapsulation for long-term stability enhancement of perovskite solar cells. *Nano Energy* **2016**, *30*, 162–172. [[CrossRef](#)]
52. Pulli, E.; Rozzi, E.; Bella, F. Transparent photovoltaic technologies: Current trends towards upscaling. *Energy Convers. Manag.* **2020**, *219*, 112982. [[CrossRef](#)]
53. Yang, C.; Liu, D.; Bates, M.; Barr, M.C.; Lunt, R.R. How to accurately report transparent solar cells. *Joule* **2019**, *3*, 1803–1809. [[CrossRef](#)]
54. Giannouli, M. Current Status of Emerging PV Technologies: A Comparative Study of Dye-Sensitized, Organic, and Perovskite Solar Cells. *Int. J. Photoenergy* **2021**, *2021*, 6692858. [[CrossRef](#)]
55. Zhou, Z.; Yuan, Z.; Yin, Z.; Xue, Q.; Li, N.; Huang, F. Progress of semitransparent emerging photovoltaics for building integrated applications. *Green Energy Environ.* **2023**. [[CrossRef](#)]
56. Inganäs, O. Organic Photovoltaics over Three Decades. *Adv. Mater.* **2018**, *30*, 1800388. [[CrossRef](#)]
57. Liu, X.; Zhong, Z.; Zhu, R.; Yu, J.; Li, G. Aperiodic band-pass electrode enables record-performance transparent organic photovoltaics. *Joule* **2022**, *6*, 1918–1930. [[CrossRef](#)]
58. Jing, J.; Dong, S.; Zhang, K.; Zhou, Z.; Xue, Q.; Song, Y.; Du, Z.; Ren, M.; Huang, F. Semitransparent organic solar cells with efficiency surpassing 15%. *Adv. Energy Mater.* **2022**, *12*, 2200453. [[CrossRef](#)]
59. Roy, A.; Sujatha Devi, P.; Karazhanov, S.; Mamedov, D.; Mallick, T.K.; Sundaram, S. A review on applications of Cu₂ZnSnS₄ as alternative counter electrodes in dye-sensitized solar cells. *AIP Adv.* **2018**, *8*, 070701. [[CrossRef](#)]
60. Richhariya, G.; Kumar, A.; Tekasakul, P.; Gupta, B. Natural dyes for dye sensitized solar cell: A review. *Renew. Sustain. Energy Rev.* **2017**, *69*, 705–718. [[CrossRef](#)]
61. Godfroy, M.; Liotier, J.; Mwalukuku, V.M.; Joly, D.; Huaulmé, Q.; Cabau, L.; Aumaitre, C.; Kervella, Y.; Narbey, S.; Oswald, F. Benzothiadiazole-based photosensitizers for efficient and stable dye-sensitized solar cells and 8.7% efficiency semi-transparent mini-modules. *Sustain. Energy Fuels* **2021**, *5*, 144–153. [[CrossRef](#)]
62. Roy, A.; Ghosh, A.; Bhandari, S.; Sundaram, S.; Mallick, T.K. Perovskite solar cells for BIPV application: A review. *Buildings* **2020**, *10*, 129. [[CrossRef](#)]
63. Yu, J.C.; Li, B.; Dunn, C.J.; Yan, J.; Diroll, B.T.; Chesman, A.S.R.; Jasieniak, J.J. High-Performance and Stable Semi-Transparent Perovskite Solar Cells through Composition Engineering. *Adv. Sci.* **2022**, *9*, 2201487. [[CrossRef](#)]
64. Bernardoni, P.; Mangherini, G.; Gjestila, M.; Andreoli, A.; Vincenzi, D. Performance Optimization of Luminescent Solar Concentrators under Several Shading Conditions. *Energies* **2021**, *14*, 816. [[CrossRef](#)]
65. Debije, M.G.; Verbunt, P.P.C. Thirty Years of Luminescent Solar Concentrator Research: Solar Energy for the Built Environment. *Adv. Energy Mater.* **2012**, *2*, 12–35. [[CrossRef](#)]

66. Slooff, L.H.; Bende, E.E.; Burgers, A.R.; Budel, T.; Pravettoni, M.; Kenny, R.P.; Dunlop, E.D.; Büchtemann, A. A luminescent solar concentrator with 7.1% power conversion efficiency. *Phys. Status Solidi (RRL)–Rapid Res. Lett.* **2008**, *2*, 257–259. [CrossRef]
67. Goldschmidt, J.C.; Peters, M.; Bösch, A.; Helmers, H.; Dimroth, F.; Glunz, S.W.; Willeke, G. Increasing the efficiency of fluorescent concentrator systems. *Sol. Energy Mater. Sol. Cells* **2009**, *93*, 176–182. [CrossRef]
68. Richter, A.; Hermle, M.; Glunz, S.W. Reassessment of the limiting efficiency for crystalline silicon solar cells. *IEEE J. Photovolt.* **2013**, *3*, 1184–1191. [CrossRef]
69. Mailoa, J.P.; Bailie, C.D.; Johlin, E.C.; Hoke, E.T.; Akey, A.J.; Nguyen, W.H.; McGehee, M.D.; Buonassisi, T. A 2-terminal perovskite/silicon multijunction solar cell enabled by a silicon tunnel junction. *Appl. Phys. Lett.* **2015**, *106*, 121105. [CrossRef]
70. Köhnen, E.; Wagner, P.; Lang, F.; Cruz, A.; Li, B.; Roß, M.; Jošt, M.; Morales-Vilches, A.B.; Topič, M.; Stolterfoht, M. 27.9% efficient monolithic perovskite/silicon tandem solar cells on industry compatible bottom cells. *Sol. RRL* **2021**, *5*, 2100244. [CrossRef]
71. Duan, L.; Walter, D.; Chang, N.; Bullock, J.; Kang, D.; Phang, S.P.; Weber, K.; White, T.; Macdonald, D.; Catchpole, K.; et al. Stability challenges for the commercialization of perovskite–silicon tandem solar cells. *Nat. Rev. Mater.* **2023**, *8*, 261–281. [CrossRef]
72. Saliba, M.; Matsui, T.; Domanski, K.; Seo, J.-Y.; Ummadisingu, A.; Zakeeruddin, S.M.; Correa-Baena, J.-P.; Tress, W.R.; Abate, A.; Hagfeldt, A. Incorporation of rubidium cations into perovskite solar cells improves photovoltaic performance. *Science* **2016**, *354*, 206–209. [CrossRef] [PubMed]
73. Domanski, K.; Correa-Baena, J.-P.; Mine, N.; Nazeeruddin, M.K.; Abate, A.; Saliba, M.; Tress, W.; Hagfeldt, A.; Grätzel, M. Not all that glitters is gold: Metal-migration-induced degradation in perovskite solar cells. *ACS Nano* **2016**, *10*, 6306–6314. [CrossRef]
74. Wang, R.; Mujahid, M.; Duan, Y.; Wang, Z.K.; Xue, J.; Yang, Y. A review of perovskites solar cell stability. *Adv. Funct. Mater.* **2019**, *29*, 1808843. [CrossRef]
75. Chen, H.; Ye, F.; Tang, W.; He, J.; Yin, M.; Wang, Y.; Xie, F.; Bi, E.; Yang, X.; Grätzel, M. A solvent-and vacuum-free route to large-area perovskite films for efficient solar modules. *Nature* **2017**, *550*, 92–95. [CrossRef] [PubMed]
76. Wang, H.; Qin, Z.; Miao, Y.; Zhao, Y. Recent Progress in Large-Area Perovskite Photovoltaic Modules. *Trans. Tianjin Univ.* **2022**, *28*, 323–340. [CrossRef]
77. Yan, J.; Savenije, T.J.; Mazzarella, L.; Isabella, O. Progress and challenges on scaling up of perovskite solar cell technology. *Sustain. Energy Fuels* **2022**, *6*, 243–266. [CrossRef]
78. Shen, H.; Walter, D.; Wu, Y.; Fong, K.C.; Jacobs, D.A.; Duong, T.; Peng, J.; Weber, K.; White, T.P.; Catchpole, K.R. Monolithic perovskite/Si tandem solar cells: Pathways to over 30% efficiency. *Adv. Energy Mater.* **2020**, *10*, 1902840. [CrossRef]
79. Babics, M.; De Bastiani, M.; Ugur, E.; Xu, L.; Bristow, H.; Toniolo, F.; Raja, W.; Subbiah, A.S.; Liu, J.; Torres Merino, L.V.; et al. One-year outdoor operation of monolithic perovskite/silicon tandem solar cells. *Cell Rep. Phys. Sci.* **2023**, *4*, 101280. [CrossRef]
80. Luo, X.; Luo, H.; Li, H.; Xia, R.; Zheng, X.; Huang, Z.; Liu, Z.; Gao, H.; Zhang, X.; Li, S. Efficient Perovskite/Silicon Tandem Solar Cells on Industrially Compatible Textured Silicon. *Adv. Mater.* **2023**, *35*, 2207883. [CrossRef]
81. VDMA. International Technology Roadmap for Photovoltaic (ITRPV), Results Including Maturity Report. 2022. Available online: <https://itrpv.vdma.org/> (accessed on 6 July 2023).
82. Han, Q.; Hsieh, Y.-T.; Meng, L.; Wu, J.-L.; Sun, P.; Yao, E.-P.; Chang, S.-Y.; Bae, S.-H.; Kato, T.; Bermudez, V. High-performance perovskite/Cu (In, Ga) Se₂ monolithic tandem solar cells. *Science* **2018**, *361*, 904–908. [CrossRef] [PubMed]
83. Jošt, M.; Köhnen, E.; Al-Ashouri, A.; Bertram, T.; Tomšič, S.P.; Magomedov, A.; Kasparavicius, E.; Kodalle, T.; Lipovšek, B.; Getautis, V. Perovskite/CIGS tandem solar cells: From certified 24.2% toward 30% and beyond. *ACS Energy Lett.* **2022**, *7*, 1298–1307. [CrossRef]
84. Singh, A.K.; Chauhan, M.S.; Patel, S.P.; Singh, R.S.; Singh, V.K. MAPbI₃-on-CuInSe₂ two-terminal monolithically integrated and four-terminal mechanically stacked tandem solar cells: A Theoretical Investigation Using SCAPS-1D. *Results Opt.* **2023**, *10*, 100358. [CrossRef]
85. Madan, J.; Singh, K.; Pandey, R. Comprehensive device simulation of 23.36% efficient two-terminal perovskite-PbS CQD tandem solar cell for low-cost applications. *Sci. Rep.* **2021**, *11*, 19829. [CrossRef]
86. Abdollahi Nejad, B.; Ritzer, D.B.; Hu, H.; Schackmar, F.; Moghadamzadeh, S.; Feeney, T.; Singh, R.; Laufer, F.; Schmager, R.; Azmi, R. Scalable two-terminal all-perovskite tandem solar modules with a 19.1% efficiency. *Nat. Energy* **2022**, *7*, 620–630. [CrossRef]
87. He, R.; Wang, W.; Yi, Z.; Lang, F.; Chen, C.; Luo, J.; Zhu, J.; Thiesbrummel, J.; Shah, S.; Wei, K. Improving interface quality for 1-cm² all-perovskite tandem solar cells. *Nature* **2023**, *618*, 80–86. [CrossRef]
88. Chen, X.; Jia, Z.; Chen, Z.; Jiang, T.; Bai, L.; Tao, F.; Chen, J.; Chen, X.; Liu, T.; Xu, X. Efficient and reproducible monolithic perovskite/organic tandem solar cells with low-loss interconnecting layers. *Joule* **2020**, *4*, 1594–1606. [CrossRef]
89. Sun, S.Q.; Xu, X.; Sun, Q.; Yao, Q.; Cai, Y.; Li, X.Y.; Xu, Y.L.; He, W.; Zhu, M.; Lv, X. All-Inorganic Perovskite-Based Monolithic Perovskite/Organic Tandem Solar Cells with 23.21% Efficiency by Dual-Interface Engineering. *Adv. Energy Mater.* **2023**, *13*, 2204347. [CrossRef]
90. NREL. Full Record of PV Cell Efficiency Data. Available online: <https://www.nrel.gov/pv/assets/docs/cell-efficiency-data-table.xlsx> (accessed on 15 June 2023).
91. Xie, M.; Liu, X.; Li, Y.; Li, X.A. Two-dimensional InSb/GaAs-and InSb/InP-based tandem photovoltaic device with matched bandgap. *Nanoscale* **2022**, *14*, 1954–1961. [CrossRef] [PubMed]
92. Werner, J.; Niesen, B.; Ballif, C. Perovskite/silicon tandem solar cells: Marriage of convenience or true love story?—An overview. *Adv. Mater. Interfaces* **2018**, *5*, 1700731. [CrossRef]

93. Li, Z.; Zhao, Y.; Wang, X.; Sun, Y.; Zhao, Z.; Li, Y.; Zhou, H.; Chen, Q. Cost analysis of perovskite tandem photovoltaics. *Joule* **2018**, *2*, 1559–1572. [[CrossRef](#)]
94. Yamamoto, K.; Mishima, R.; Uzu, H.; Adachi, D. High efficiency perovskite/heterojunction crystalline silicon tandem solar cells: Towards industrial-sized cell and module. *Jpn. J. Appl. Phys.* **2023**, *62*, SK1021. [[CrossRef](#)]
95. Green, M.A. Commercial progress and challenges for photovoltaics. *Nat. Energy* **2016**, *1*, 15015. [[CrossRef](#)]
96. Martinho, F. Challenges for the future of tandem photovoltaics on the path to terawatt levels: A technology review. *Energy Environ. Sci.* **2021**, *14*, 3840–3871. [[CrossRef](#)]
97. NEXUS Project: Next Generation of Sustainable Perovskite-Silicon Tandem Cells. Available online: <https://nexus-pv.eu/> (accessed on 14 July 2023).
98. 4SUNS Project: 4-Colours/2-Junctions of III-V Semiconductors on Si to Use in Electronics Devices and Solar Cells. Available online: <https://cordis.europa.eu/project/id/758885> (accessed on 12 July 2023).
99. Chatzipanagi, A.; Jaeger-Waldau, A.; Cleret, D.; Letout, S.; Latunussa, C.; Mountraki, A.; Georgakaki, A.; Ince, E.; Kuokkanen, A.; Shtjefni, D. *Clean Energy Technology Observatory: Photovoltaics in the European Union—2022 Status Report on Technology Development, Trends, Value Chains and Markets*; Publications Office of the European Union: Luxembourg, 2022.

Disclaimer/Publisher’s Note: The statements, opinions and data contained in all publications are solely those of the individual author(s) and contributor(s) and not of MDPI and/or the editor(s). MDPI and/or the editor(s) disclaim responsibility for any injury to people or property resulting from any ideas, methods, instructions or products referred to in the content.